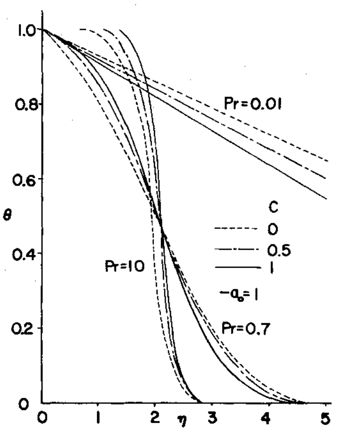

Fig. 2 Dimensionless temperature profiles for $A_0 = -1$.

this condition, the thermal boundary-layer thickness is much greater than that of the velocity boundary layer and the usual boundary-layer approximation implicit in Eq. (3) may become poor.

The heat flux at the surface is given by

$$q_w = -k\left.\frac{\partial T}{\partial y}\right|_{y=0} = -k(T_w - T_\infty)\left(\frac{K_x}{\nu}\right)^{1/2}\theta'(0) \tag{21}$$

Introducing the Nusselt number

$$Nu = \frac{q_w(xU_\infty/K_x)^{1/2}}{k(T_w - T_\infty)}$$

and the Reynolds number $Re = xU_\infty/\nu$, Eq. (21) may be rewritten as

$$Nu/Re^{1/2} = -\theta'(0) \tag{22}$$

The value of $Nu/Re^{1/2}$ increases with increasing C for fixed value of $-A_0$ and Prandtl number. The transpiration cooling becomes the more effective, the larger the Prandtl number becomes and for fixed value of C, the effectiveness of the blowing in reducing the heat transfer will become more prevalent when the Prandtl number increases.

References

[1] Hartnett, J. P. and Eckert, E. R. G., "Mass-Transfer Cooling in a Laminar Boundary Layer With Constant Fluid Properties," *Transactions of the ASME*, Vol. 79, 1957, pp. 247–254.

[2] Sparrow, E. M., Eckert, E. R. G., and Minkowyez, W. J., "Transpiration Cooling in a Magnetohydrodynamic Stagnation Point Flow," *Applied Scientific Research*, Sec. A, Vol. 11, 1962, pp. 125–147.

[3] Howarth, L., "The Boundary Layer in Three Dimensional Flow," Pt. I, "Derivation of the Equations for Flow Along a General Surface," *Philosophical Magazine*, Vol. 7s, No. 42, 1951, pp. 239–244.

[4] Howarth, L., "The Boundary Layer in Three Dimensional Flow," Pt. II, "The Flow Near a Stagnation Point," *Philosophical Magazine*, Vol. 7s, No. 42, 1951, pp. 1433–1440.

Droplet Dynamics in a Hypersonic Shock Layer

N. A. JAFFE*
Acurex Corp./Aerotherm Division, Mountain View, Calif.

Introduction

HYPERSONIC vehicles may encounter condensed water vapor in the form of either ice particles or liquid droplets. Particle deceleration and ablation effects in the shock layer were

Received February 26, 1973; revision received June 18, 1973.
Index category: Fluid Dynamics, Thermophysics and Thermochemistry.

* Staff Engineer.

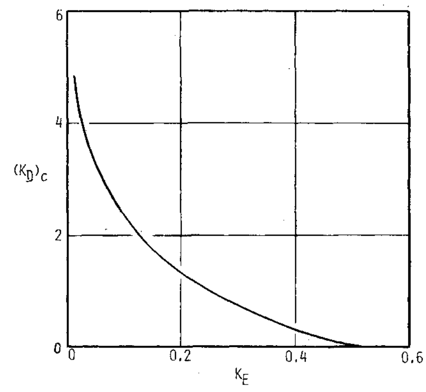

Fig. 1 Critical ablation curve.

considered by Waldman and Reinecke.[1] These effects are coupled; however, in Ref. 1 velocities employed in the energy equation were taken from a constant mass solution to the momentum equation. In addition, the heat transfer in Ref. 1 was scaled with the particle velocity cubed (U^3). One stated objective was to obtain closed form solutions; however, only numerical solutions were obtainable for the energy equation. If the equations are treated in a coupled manner, closed form solutions are obtainable for both momentum and energy equations. It is felt that scaling the heat transfer as U^3 leads to even more serious errors than neglect of coupling. This scaling was adopted in order to relate the over-all heat-transfer rate, to the particle, to its stagnation value. This treatment is valid for a body in a cold freestream; in the limit it yields the result that there is no heat transfer to a cold particle stationary in the shock layer, relative to the vehicle. References 2–4 indicate that particle heating rates can be expressed in terms of a mean temperature drop ΔT_m, and Nusselt number Nu_m over a wide range of conditions for subsonic and supersonic flow and a much weaker dependence on velocity than is employed in the model used in Ref. 1. Indeed the Nusselt number variation is small over a Reynolds number range of several orders of magnitude.[4] Thus, in the present analysis the heat transfer is modeled with a Nusselt number and the equations remain coupled.

Analysis

The energy equation for a particle of mass m, can be written

$$Q^*(dm/dt) = -\dot{Q} \tag{1}$$

The quantities $\dot{Q}$ and Q^* are the net heat rate (average heat flux x area) to the particle and the particle effective heat of ablation. The momentum equation along the stagnation streamline is

$$m(dU/dt) = -\tfrac{1}{2}C_D A\rho_s U^2 \tag{2}$$

where C_D is the particle drag coefficient based on cross-sectional area A; σ and ρ_s are particle and shock layer densities. The preceding equations are written in a coordinate system fixed with respect to the vehicle. It is assumed that the gas velocity in the shock layer is negligible compared to the particle velocity. If mass loss is assumed to take place as a result of fusion then Q^* must include the latent heat of fusion; if vaporization is the mechanism for mass loss then the heat of vaporization must also be included. Equation (1) implies that potential rate controlling processes such as phase change kinetics and diffusion have been neglected; thus, the results of the analysis represent a bounding case for mass transfer effects.

The equations are subsequently written for a spherical particle of radius r. The quantity $\dot{Q}$ is written in terms of a mean heat-transfer coefficient h_m and temperature drop ΔT_m

$$\dot{Q} = 4\pi r^2 h_m \Delta T_m \tag{3}$$

where

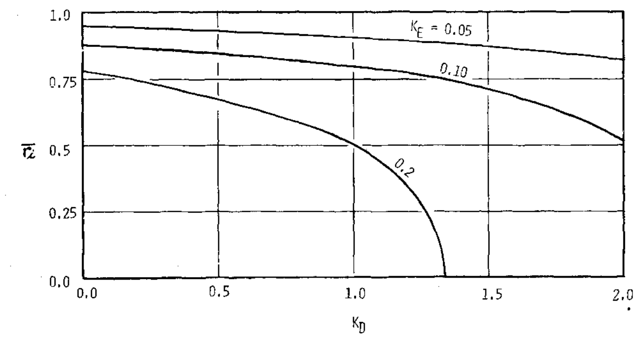

Fig. 2 Particle impact radius.

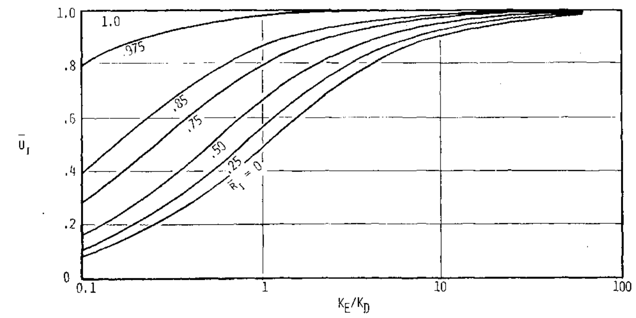

Fig. 4 Particle impact velocity.

$$h_m = k_m Nu_m/2r$$

Substituting the preceding into Eq. (1), introducing dimensionless coordinates, and replacing the independent variable time with distance from the shock layer, yields

$$d\bar{U}/d\bar{x} = -K_D \bar{U}/\bar{r} \tag{4}$$

$$d\bar{r}/d\bar{x} = -K_E/\bar{U}\bar{r} \tag{5}$$

where

$$d\bar{x} = \bar{U}\, d\bar{t} \tag{6}$$

$$K_D = 3/8 C_D (\rho_s/\sigma) \Delta_s/r_e \tag{7}$$

$$K_E = k_m Nu_m \Delta T_m \Delta_s/2\sigma Q^* U_\infty r_e^2 \tag{8}$$

Velocities and distances have been nondimensionalized with respect to freestream velocity U_∞, and shock layer thickness Δ_s; particle radius has been nondimensionalized with respect to its freestream value r_e. The initial conditions on Eqs. (4–6) are

$$\bar{U} = \bar{r} = 1 \text{ at } \bar{x} = \bar{t} = 0$$

The equations have been written for spherical particles, the dimensionless form is not quite that restrictive. If drag and heat transfer are modeled correctly they are valid for irregular shapes, providing mass scales as r^3 and area as r^2. For fixed particle size, Mach number, vehicle nose radius, and altitude, K_D and K_E are relatively constant. Strictly speaking, there will be some variation of these quantities with $\bar{r}$ and $\bar{U}$ which could be included in the analysis. In view of uncertainties associated with actual particle geometries and, consequently, their heat-transfer and drag coefficients this refinement is unwarranted.[5]

The coupled solution to Eqs. (4–6), subject to the aforementioned initial conditions is

$$\bar{x} = \frac{1}{K_D}\left\{(\bar{r}-1)+\left(1+\frac{K_E}{K_D}\right)\ln\left[1-\frac{K_D}{K_E}(\bar{r}-1)\right]\right\} \tag{9}$$

$$\bar{U} = [(1+K_D/K_E)-(K_D/K_E)\bar{r}]^{-1} \tag{10}$$

and

$$\bar{r} = (1-2K_E\bar{t})^{1/2} \tag{11}$$

The condition for total mass loss is obtainable from Eq. (9) with $\bar{r} = 0$ at $\bar{x} = 1$, yielding a relationship between K_E and a critical $(K_D)_c$, shown in Fig. 1. Points above this curve represent conditions for which the particle will not survive to impact the vehicle. Figure 2 illustrates effects of K_D and K_E on particle impact radii $\bar{r}_i$ ($\bar{r}$ at $\bar{x} = 1$). Figure 3 illustrates radius histories for surviving ($\bar{r} > 0$ at $\bar{x} = 1$) and nonsurviving $\bar{r} = 0$ at $\bar{x} < 1$) particles. Impact velocities are represented parametrically in Fig. 4.

Discussion

The present results indicate that drag and aeroheating effects reinforce each other in relation to particle deceleration and ablation in the shock layer. These results are in contrast to those given in Ref. 1. In Ref. 1 it is assumed that only the upstream portion of the particle is heated, the heat transfer is expressible in terms of a fraction of the stagnation point heating, with a $\bar{U}^3$ correction for deceleration effects, yielding

$$\dot{Q} = 2\pi r^2[(0.53)q_s]\bar{U}^3 \tag{12}$$

where $q_s = E/r^{1/2}$ and E is related to freestream density and Mach number. Furthermore, $\bar{U}^3$ was obtained from the constant radius solution to Eq. (4), $\bar{U} = e^{-K_D\bar{x}/\bar{r}}$, yielding the dimensionless energy equation

$$\bar{r}^{1/2}\, d\bar{r}/d\bar{x} = -0.265 H_e e^{-2K_D\bar{x}/\bar{r}} \tag{13}$$

where

$$H_e = E\Delta_s/\sigma Q^* U_\infty r_e^{3/2}$$

Results of a numerical solution to Eq. (13) from Ref. 1 are reproduced in Fig. 5 for the purpose of comparison. It is pointed out that a closed form solution is obtainable, even within the framework of assumptions used in Ref. 1, had the equations been allowed to remain coupled.[5]

Figures 2 and 5 illustrate that increasing the dimensionless energy parameters K_E or H_e promotes mass loss; however the effects of K_D are not in agreement. Reference 1, as a consequence of the heat-transfer model used, indicates that drag and heating effects oppose each other, insofar as particle ablation is concerned. Increasing drag, decreases particle velocity and hence ablation, since heating was scaled as U^3. In the present model,

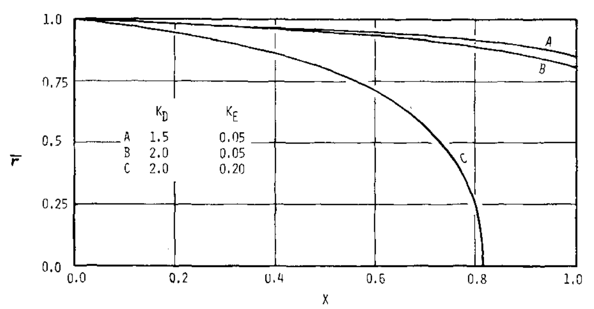

Fig. 3 Particle radius profiles.

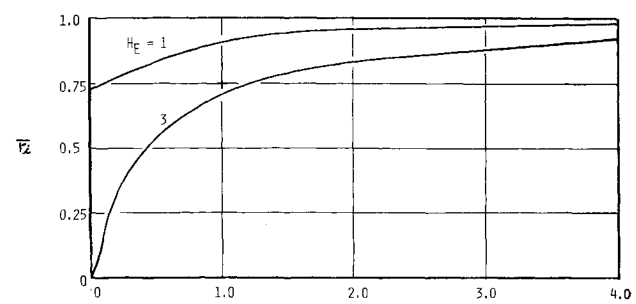

Fig. 5 Particle impact radius (from Ref. 1).

drag effects reinforce mass loss in that the amount of ablation increases with particle residence time (not velocity) in the shock layer. From Eq. (11) it can be seen that K_E is a dimensionless measure of the ratio of particle residence time in the shock layer to ablation time. For $K_E = 1/2$, $\bar{t} = t/(\Delta_s/U_\infty) = 1$, corresponds to the time required for complete ablation. This is deducible from Fig. 1 which shows that for zero drag ($K_D = 0$), no particles with values of $K_E \geqq 1/2$ survive; this value can be used to determine the largest size particle that will not survive. That is [see Eq. (8)] particles satisfying the condition

$$r_e \leqq (k_m Nu_m \Delta T_m \Delta_s/\sigma Q^* U_\infty)^{1/2}$$

would be predicted not to survive the shock environment. The reinforcing effects are expected to be a strong function of r_e since K_D varies as r_e^{-1} and K_E as r_e^{-2}. For very low velocities and small particle radii the analysis becomes invalid due to the fact that the gas velocity has been assumed negligible relative to the particle velocity and the assumption of constant drag coefficient break down. Nevertheless, this should cause the predictions to be conservative since the drag coefficient increases as particle Reynolds number goes to zero. As was pointed out the model used is idealized in that diffusion and phase change kinetics have been ignored; thus the results are representative of a bounding case. A more detailed treatment is given in Ref. 5.

References

[1] Waldman, G. D. and Reinecke, W. G., "Particle Trajectories, Heating and Breakup in Hypersonic Shock Layers," *AIAA Journal*, Vol. 9, No. 6, June 1971, pp. 1040–1048.

[2] Hoglund, R. F., "Recent Advances In Gas-Particle Nozzle Flows," *ARS Journal*, Vol. 32, 1962, pp. 662–671.

[3] Gilbert, M., Allport, J., and Dunlap, R., "Dynamics of Two-Phase Flow in Rocket Nozzles," *ARS Journal*, Vol. 32, 1962, pp. 1929–1930.

[4] Carlson, D. J. and Hoglund, R. F., "Particle Drag and Heat Transfer in Rocket Nozzles," *AIAA Journal*, Vol. 2, No. 11, Nov. 1963, pp. 1980–1984.

[5] Jaffe, N. A., "Particle Deceleration and Heating In a Hypersonic Shock Layer," TN-73-18, Feb. 1973, Aerotherm, Mountain View, Calif.

Inviscid Swirling Flows through a Choked Nozzle

C. T. Hsu* and A. D. DeJoode†

Iowa State University, Ames, Iowa

FOR a steady, inviscid, isoenergetic and homentropic, swirling flow through a circular, constant-area pipe, the radial distribution of axial Mach number was obtained[1,2] previously in closed form solutions as follows:

$$M_a^2 = C_1/\{1-(\alpha^2R^2)/r^2-[(\gamma-1)/2]C_1\} \tag{1}$$

for a free-vortex flow in which the tangential velocity decreases inversely with radial distance, and

$$\frac{[1+(\gamma-1)M_a^2/2]}{[1+(\gamma-1)M_a^2/4]} = C_2[1-(\gamma-1)\omega^2r^2/2a_o^2] \tag{2}$$

for a forced-vortex flow in which the tangential velocity increases linearly with radial distance, where

$$\alpha(r) = [(\gamma-1)/2]^{1/2}\Gamma/a_o R \tag{3}$$

is the swirling parameter. C_1 and C_2 are two arbitrary constants to be determined; r denotes the radial distance; R, the radius of the pipe; γ, the ratio of specific heats; ω, the angular velocity of solid body rotation; a_o, the stagnation sound speed; and $\Gamma = vr$, the circulation per unit radian evaluated at various radial distances.

In a real nozzle flow, a Rankine-combined vortex, i.e., a forced vortex core of radius r_c with outer free-vortex flow is more likely[3] to occur. In this case, superposition of these two types of vortex flows can be directly obtained from Eqs. (1) and (2). Then, the mass flow rate can also be superimposed for a given stagnation pressure p_o, a stagnation temperature T_o, and the pipe area, as follows:

$$\dot{m}(\alpha_c, r_c, C_1, C_2) = \dot{m}_1(\alpha_c, r_c, C_1) + \dot{m}_2(\alpha_c, r_c, C_2) \tag{4}$$

where

$$\dot{m}_1 = 2\pi p_o\left(\frac{\gamma C_1}{R'T_o}\right)^{1/2}\int_{r_c}^{R}\left[1-\frac{\alpha_c^2R^2}{r^2}-\frac{\gamma-1}{2}C_1\right]^{1/(\gamma-1)} r\,dr \tag{4a}$$

represents the portion of free vortex flow, R' is the gas constant, and where

$$\dot{m}_2 = 4\pi p_o[\gamma/(\gamma-1)R'T_o]^{1/2}C_2^{(\gamma+1)/(2-2\gamma)}\int_0^{r_c}\left[2-C_2\times\left(1-\frac{\alpha_c^2r^2R^2}{r_c^4}\right)\right]^{1/(\gamma-1)}\left[C_2\left(1-\frac{\alpha_c^2r^2R^2}{r_c^4}\right)-1\right]^{1/2} r\,dr \tag{4b}$$

represents the portion of forced vortex core flow, where

$$\alpha_c = \left(\frac{\gamma-1}{2}\right)^{1/2}\frac{\omega r_c^2}{a_o R} = \left[\frac{\text{max. swirl energy}}{\text{total energy}}\right]^{1/2}\frac{r_c}{R} \tag{5}$$

is now the maximum swirling parameter evaluated at r_c. Also, at r_c, M_a is continuous, so C_1 is related to C_2 from Eqs. (1) and (2) by

$$C_1 = 4\left[C_2\left(1-\frac{\alpha_c^2R^2}{r_c^2}\right)-1\right]\Big/(\gamma-1)C_2 \tag{6}$$

When $\dot{m}$ is choked at the pipe or delivers the maximum mass flow rate for a given α_c and r_c, the complete flow nature in the pipe can be determined by obtaining C_1 or C_2 from the choking condition,

$$\partial\dot{m}/\partial C_1 = 0 \quad \text{or} \quad \partial\dot{m}/\partial C_2 = 0 \tag{7}$$

The following examples were evaluated by numerical computations for C_1 or C_2 from Eq. (7), i.e., to find a range of C_1

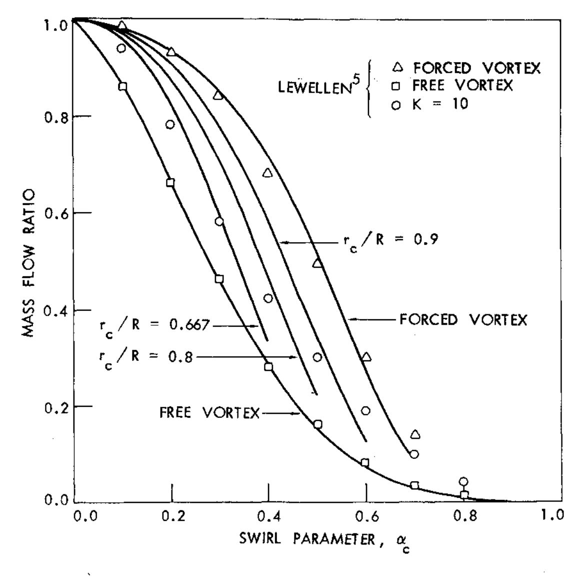

Fig. 1 Choked mass flow ratio vs swirl parameter.

Received February 28, 1973; revision received May 25, 1973. This research was supported by the Engineering Research Institute, Iowa State University.

Index category: Nozzle and Channel Flow.

* Professor, Department of Aerospace Engineering, and Engineering Research Institute. Member AIAA.

† Formerly graduate student, Department of Aerospace Engineering; now with Rockwell International, Columbus, Ohio. Associate Member AIAA.